Review

Catalytic Degradation of Nerve Agents

Agatino Zammataro [1], **Rossella Santonocito** [1], **Andrea Pappalardo** [1,2] **and**
Giuseppe Trusso Sfrazzetto [1,2,*]

[1] Department of Chemical Sciences, University of Catania, Viale Andrea Doria 6, 95125 Catania, Italy;
agatino.zammataro@studium.unict.it (A.Z.); santonocito.rossella@studium.unict.it (R.S.);
andrea.pappalardo@unict.it (A.P.)

[2] INSTM Udr of Catania, Viale Andrea Doria 6, 95125 Catania, Italy

* Correspondence: giuseppe.trusso@unict.it; Tel.: +39-095-7385-201

Abstract: Nerve agents (NAs) are a group of highly toxic organophosphorus compounds developed before World War II. They are related to organophosphorus pesticides, although they have much higher human acute toxicity than commonly used pesticides. After the detection of the presence of NAs, the critical step is the fast decontamination of the environment in order to avoid the lethal effect of these organophosphorus compounds on exposed humans. This review collects the catalytic degradation reactions of NAs, in particular focusing our attention on chemical hydrolysis. These reactions are catalyzed by different catalyst categories (metal-based, polymeric, heterogeneous, enzymatic and MOFs), all of them described in this review.

Keywords: Chemical Warfare Agents; catalytic degradation; metal catalysts; MOFs; enzymes

1. Introduction

Incidents involving chemical weapons, including terrorist attacks, are one of the most dangerous threats in the modern international scenario [1,2]. In fact, in the recent past, reports from the Middle East highlight the wide use of chemical weapons [3], also called Chemical Warfare Agents (CWAs) or Nerve Agents (NAs), as terrorist tool.

In general, a terrorist attack by using NAs could be performed by releasing a toxic chemical weapon in the air [4], by nebulization of the liquid or vaporization of a volatile molecule, or in water [5], by dissolving the toxic compound in the water system. In these cases, the first step will be the fast detection of the NAs [6,7], briefly shown below, followed by the prompt execution of the appropriate decontamination protocols. These protocols are based on chemical reactions by using different types of reactions, such as acid/basic conditions metal-catalyzed, polymeric/heterogeneous catalysis, enzymatic catalysis or reaction by Metal–Organic Framework (MOF). In particular, these methods allow increasing the catalytic degradation/hydrolysis rate of different order of magnitude respect to the uncatalyzed reactions. Some recent reviews summarize neutralization methods based on organocatalysts and oxidation reactions [8], polyoxometalates (POM) [8], MOF [9–12], continuous flow [8] and enzymatic reactions [13]. After a brief overview on the definition of NAs, their toxicity and detection methods, the objective of this review is to summarize the decontamination protocols able to destroy these toxic compounds, thereby restoring normal safety conditions, based on the hydrolysis reactions catalyzed by: (i) metal catalysts; (ii) polymeric/heterogeneous systems; (iii) enzymes; and (iv) MOFs [14,15]. Our attention is focused on protocols using homogeneous and heterogeneous catalytic reactions, applied both in solution and in the gaseous phase.

2. Definition of NAs

NAs are today classified into three main classes: G-type, V-type [16] and, the most recent, A-type (also called Novichok) (Figure 1) [17,18].
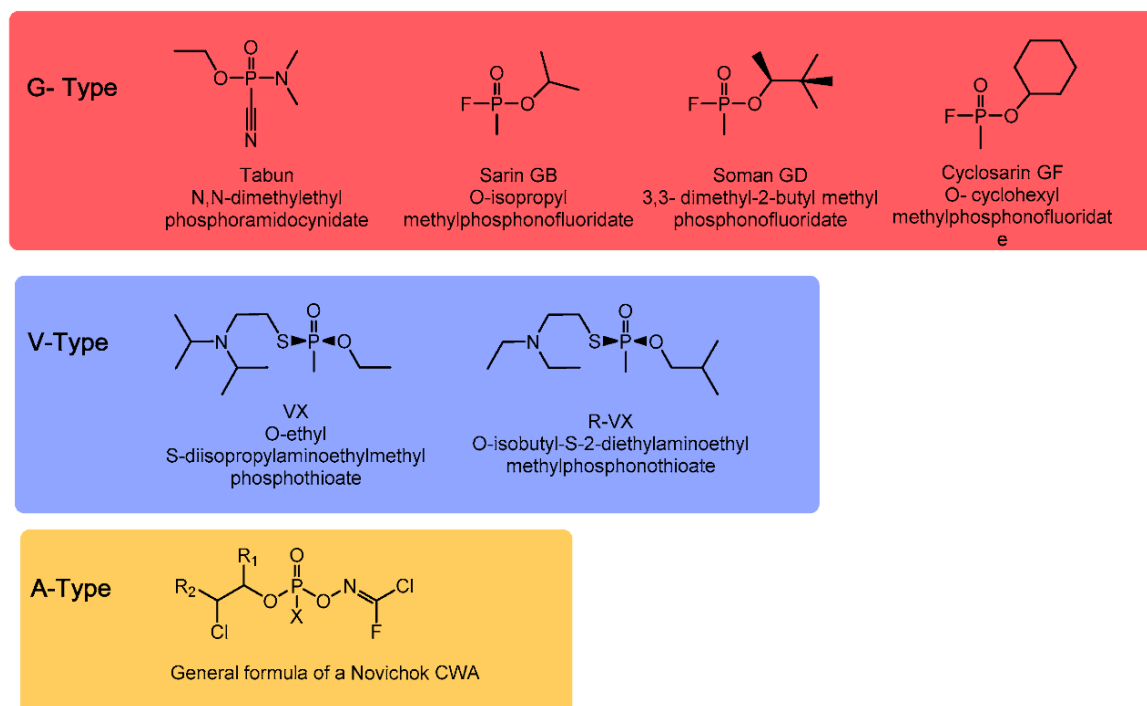

Figure 1. Structures and names of G-type, V-type and general formula of A-type Nerve Agents (NA) (adapted with permission from *Chem. Rev.* **2015**, *115*, PR1–PR76. Copyright 2015 American Chemical Society).

The first generation of NA, also called "G-Type" (German-agents), was discovered in the late 1930s and early 1940s. They include the Cyanophosphoramidate [19], Tabun (GA) [20] and methylfluorophosphonates compounds, such as Sarin (GB) [21], Soman (GD) [22] and Cyclosarin (GF) [23] (Figure 1).

After World War II, methylphosphothioates, called V-Type (venomousagents), were discovered: VX [24] (in Great Britain) and RVX [25] (the related Russian isomer). V-agents differ from G-agents by their lower volatility, their higher persistency in the environment and thus their higher toxicity.

All these organophosphorus (OP) compounds share a common chemical structure, in which a phosphorous (V) is bonded with a terminal oxide and three singly bonded substituents (where, in general, one is a good leaving group). For research activity, NAs cannot be used for safety and security reasons. Thus, the development of efficient catalytic degradation systems is performed by using simulants. These are organophosphorus compounds having similar chemical-physical characteristics as the NAs, but which are less reactive and thus less toxic [26,27]. The reduced toxicity can be ascribed to the absence of a good leaving group, avoiding the nucleophilic attack of the natural enzyme (vide infra). These compounds, summarized in Chart 1, can be classified into three classes: phosphonic ester (in blue), methylphosphonate (in green) and phosphothionate (in red).
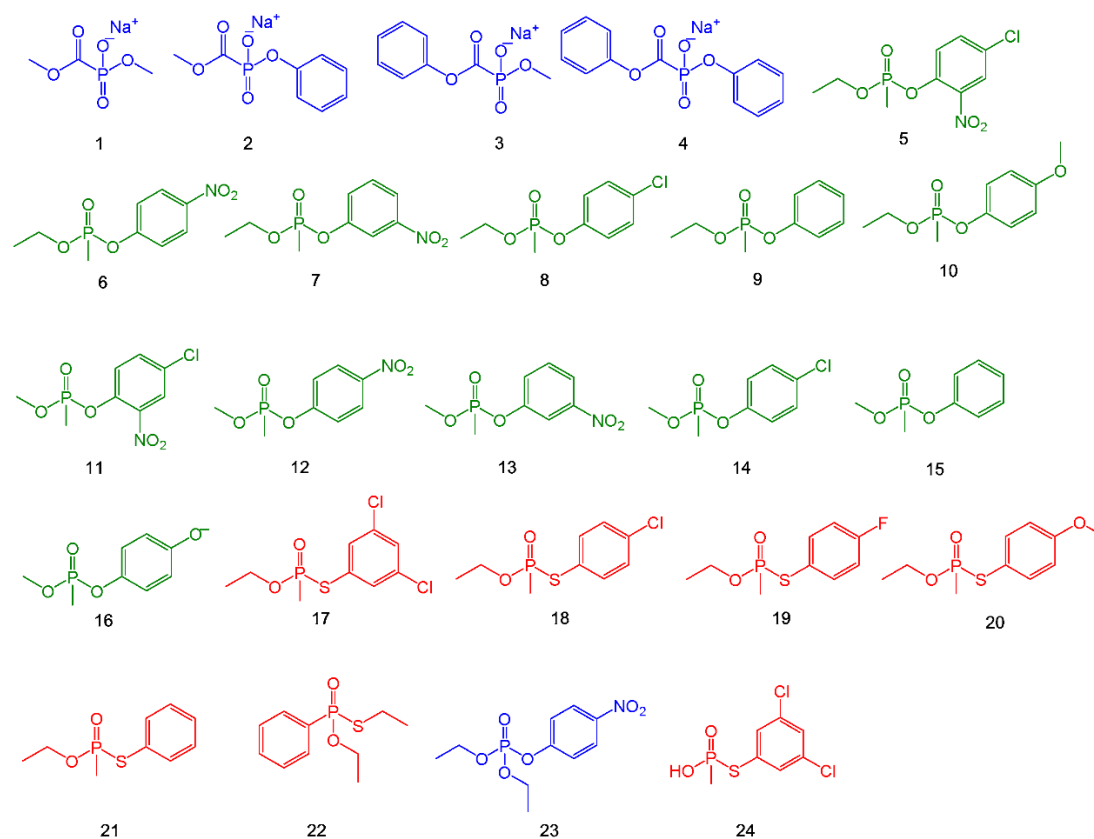
Chart 1. Chemical structure of NAs simulants used in the catalytic degradation.

Table 1 summarizes the main physical characteristics of some NAs. These compounds show volatility values comparable to water, at room temperature, thus the main method for dispersing these compounds is by aerosol, as a recent terrorist attack on the Tokyo subway demonstrated [28]. Another crucial parameter is the persistency, defined as the ability of the NA to remain active in the environment [29]. In particular, this parameter is due to the combination of the volatility, density and stability with light and water exposure. In general, as reported in Table 1, V-Type NAs show higher persistency relative to G-Type NAs due to the higher vapor pressure and volatility.

Table 1. Physical properties of NAs.

	Vapor Pressure	Volatility	Odor	Solubility	Persistency
Tabun (GA) CAS#77-81-6	0.037 mm Hg at 20 °C	576–610 mg/m^3 at 25 °C	Fruity	9.8 g/100 g at 25 °C	$T_{1/2}$ = 24–36 h
Sarin (GB) CAS#107-44-8	2.1 mm Hg at 20 °C	16,400–22,000 mg/m^3 at 25 °C	Odorless	Miscible	2–24 h at 5–25 °C
Soman CAS#96-64-0	0.40 mm Hg at 20 °C	3060–3900 mg/m^3 at 25 °C	Fruity; oil of camphor	2.1 g/100 g at 20 °C	Relatively persistent
GF CAS#329-99-7	0.07 mm Hg at 25 °C	59 ppm	Odorless	3.7 g/100 g at 25 °C	Unknown
VX CAS#20820-80-8	0.0007 mm Hg at 20 °C	3–30.0 (10.5) mg/m^3 at 25 °C	Odorless	Miscibile at <9.4 °C "Slight" at 25 °C	2–6 days

3. Toxicity of NAs

The high toxicity of OP compounds is due to their rapid inhibition of AChE (Acetylcholinesterase) in the human synapses, leading to an accumulation of acetylcholine, resulting in permanent saturation of muscarinic and nicotinic receptors, which leads to cholinergic crisis [30].

The mechanism of AChE inhibition by NAs is similar to the hydrolysis of acetylcholine catalyzed by the serine–histidine–glutamate triad in the active site of the enzyme [22,31]. In the first step of the hydrolysis, nucleophilic serine attacks acetylcholine to form a tetrahedral transition state, which evolves with the release of choline (Scheme 1A). In the second step, a water molecule activated by the nearby histidine attacks the acetylserine, leading to the formation of a second tetrahedral transition state that collapses to the free enzyme and acetic acid.
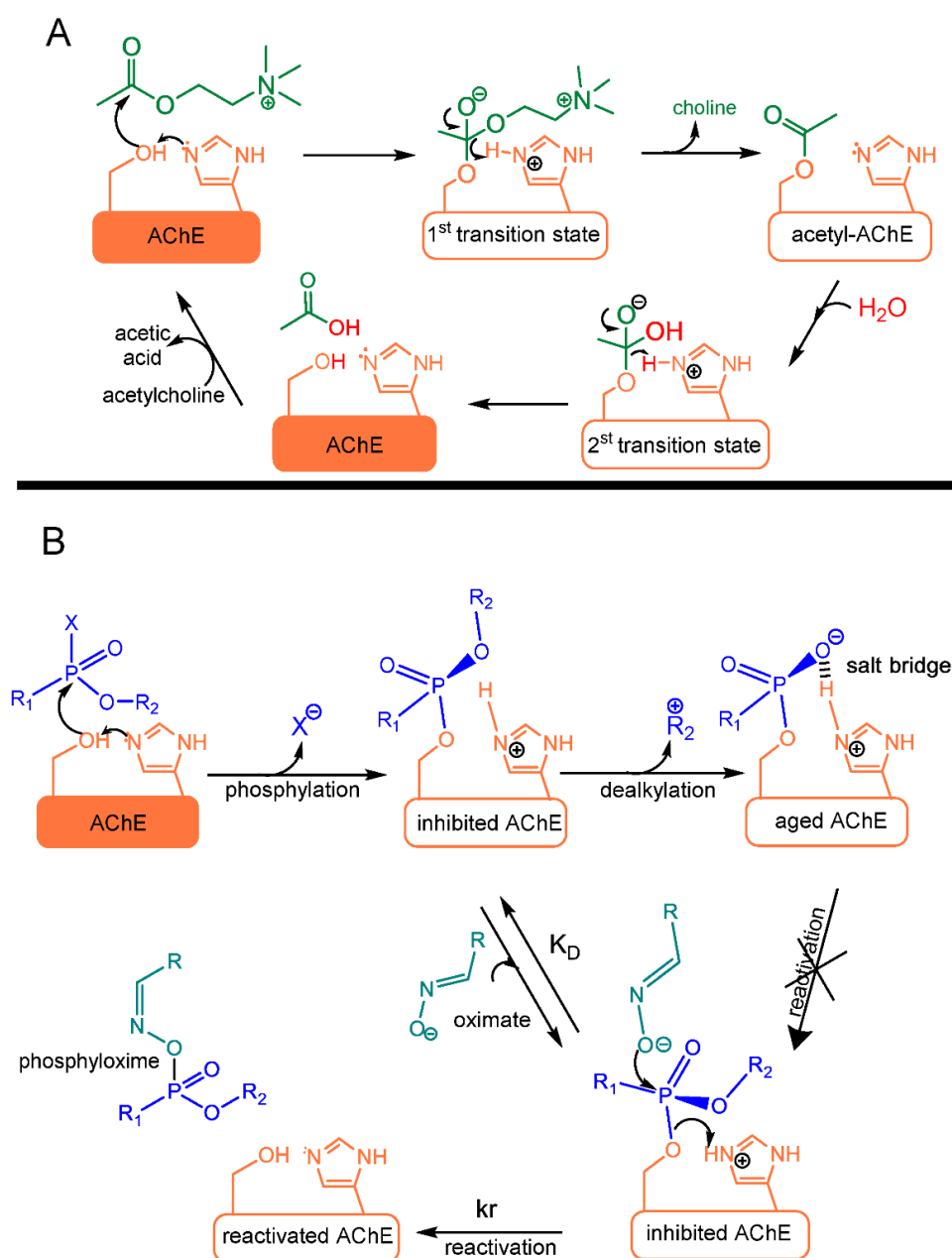
Scheme 1. (**A**) Mechanism of acetylcholine hydrolysis by AChE; and (**B**) mechanism of AChE inhibition by organophosphorus nerve agents, aging, and reactivation by oximate (adapted with permission from *Acc. Chem. Res.* **2012**, *45*, 756–766. Copyright 2012 American Chemical Society).

In the presence of a NA compound, after reaching the active site of AChE enzyme, the OH group of serine attacks the phosphorous atom, resulting in the elimination of the leaving group (Scheme 1B). The covalent adduct is similar to the transition state of the initial step of hydrolysis of acetylcholine. However, in the second step, the histidine residue in the catalytic site cannot activate the water molecule because it is in a salt-bridge with an anionic intermediate obtained after the dealkylation. For this reason, the spontaneous hydrolysis of the adduct phosphyl-enzyme (aged-enzyme) is extremely slow, varying from hours for dimethyl phosphoryl conjugates to days for V-agent AChE conjugates [32].

The presence of oximate (acting as an antidote) can prevent the dealkylation reaction due to the nucleophilic attack of the oximate anion to the phosphorous atom, leading to the phosphyloxime and restoring the natural form of the enzyme [33]. Following the reactions reported in Scheme 1, it is evident that the administration of oximate to restore the enzyme must be done as soon as possible, in order to avoid the dealkylation reaction and the "aging" of the enzyme. The aging time varies from minutes (Soman), to hours (Sarin), or days (VX and Tabun show aging time of ca. 40 h) [34–36].

The clinical manifestations after the exposure to NAs are wide [37,38]. They include salivation, lacrimation, urination, defecation, diaphoresis, gastric emesis, bronchorrhea, bronchoconstriction and bradycardia (muscarinic manifestations). Additional severe effects are related to the inhibition of nicotinic transmitters, such as fasciculations, weakness and facial paralysis. Furthermore, lethal nicotinic effects include the paralysis of the diaphragm and muscles of the chest wall.

Table 2 reports the toxicity levels of the common NAs.

Table 2. Toxicity values of some NAs.

	LD_{50} (Percutaneous)	LC_{50}	LCt_{50}	IDLH [39]
Tabun (GA) CAS#77-81-6	1 gm/person	2 ppm	100–400 mg × min/m^3	0.03 ppm
Sarin (GB) CAS#107-44-8	1.7 gm/person	1.2 ppm	50–100 mg × min/m^3	0.03 ppm
Soman CAS#96-64-0	0.35 gm/person	0.9 ppm	25–70 mg × min/m^3	0.008
GF CAS#329-99-7	0.03 gm/person	Unknown	Unknown	Unknown
VX CAS#20820-80-8	0.01 gm/person	0.3 ppm	5–50 mg × min/m^3	0.002 ppm

Nerve agents are among the most lethal agents available that have been developed for military use. The percutaneous LD_{50}, or dose required to kill 50% of those exposed, is in the milligram range for many agents. A drop of VX on the skin is potentially lethal. The concentration-time product is a measure of exposure to a vapor or aerosol over time. The LCt_{50} is the concentration-time product that is lethal to 50% of those exposed and reflects toxicity by inhalation route. IDLH. The IDLH is the concentration of toxin in air that is "immediately dangerous to life and health". For VX vapor in air, 2 parts per billion is likely to result in toxicity (adapted with permission from *Chem. Rev.* **2015**, *115*, PR1−PR76. Copyright 2015 American Chemical Society).

4. Detection of Nerve Agents

In general, the detection of G- and V-type NAs is based on an instrumental method, such as ESI-MS [40], HPLC-MS [41] or GC-MS [42]. These techniques are very sensitive and selective, but have the disadvantage of not being able to be performed in real-time, due to instrumental dimensions. An efficient alternative detection method is based on "molecular sensors", in which a molecule reacts/interacts with the analyte, giving a change of a measurable response (i.e., electrical, optical or magnetic response) [43]. In this context, NAs detection via molecular sensors is based on a "*covalent approach*", in which a covalent reaction occurs between the sensor and the analyte, leading to the formation of a new compound having different properties with respect to the starting sensor (Figure 2A) [44]. In particular, detection methods based on spectroscopic measurements (e.g., optical measurements, such as absorbance or fluorescence) are cheap and convenient, due to fast and clear

visible responses to the presence of the analyte [45]. However, the covalent approach suffers from certain limitations: (1) low selectivity, due to the possibility of reaction with other substances; and (2) one-time use, due to the covalent and irreversible reaction with the analyte.
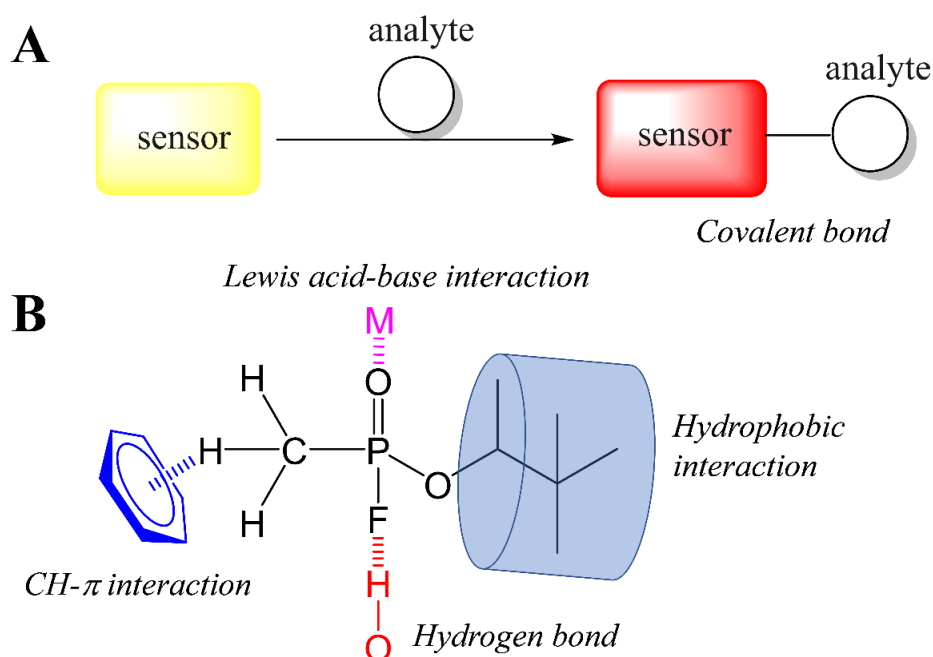

Figure 2. (**A**) Covalent approach; and (**B**) supramolecular approach used with chemical sensor for the detection of NAs.

Recently, an alternative detection method based on the formation of non-covalent interactions between the sensor and the analyte has been proposed. Due to the nature of these non-covalent interactions, this strategy is called "*supramolecular approach*" [46]. The goal of the supramolecular approach is to give alternative pathways with respect to the traditional chemical reactivity, minimizing or eliminating the effects due to the presence of competitive analytes, leading to a reusable sensor. In fact, the formation of non-covalent interactions leads to a reversible complex with the analyte [47–59].

In this context, by taking advantage of the most recent findings in the field of supramolecular chemistry, sensing devices for the non-covalent detection of CWA molecules via a "*multi-topic approach*" have been synthesized [60–65]. In particular, the target is to recognize CWAs via non-covalent reversible interactions, involving different recognition sites (multi-topic) of the analyte. The possibility of simultaneously recognizing two or more sites of the analyte leads to highly efficient and selective sensors, avoiding false-positive responses (Figure 2).

5. Chemical Hydrolysis

5.1. Metal-Catalyzed Hydrolysis

The catalytic systems described in this paragraph can be rationalized by use of two possible reaction mechanisms: a mono-metallic and a bi-metallic mechanism (Scheme 2). In many cases, the bi-metallic mechanism is utilized, simulating the catalytic activity of enzymes, where more than one Lewis acid center is present in the active site.
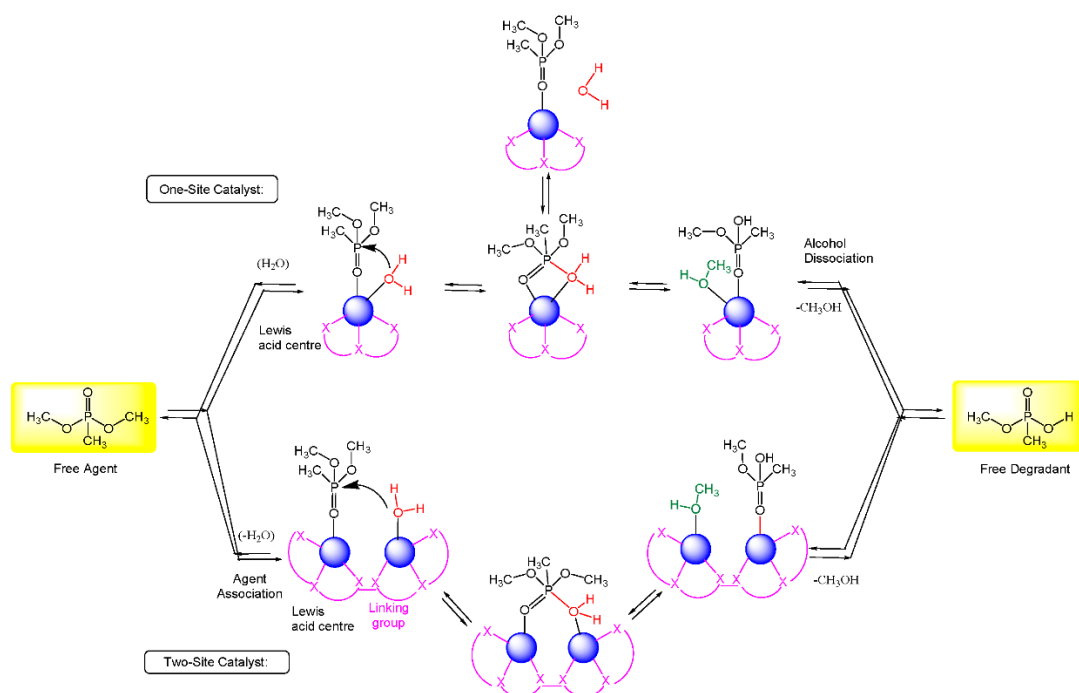
Scheme 2. Hydrolysis or methanolysis by mono-metallic or bi-metallic mechanisms (adapted with permission from *Chem. Rev.* **2015**, *115*, PR1−PR76. Copyright 2015 American Chemical Society).

Moss et al. reported the chemoselective metal-catalyzed hydrolysis of some phosphonoformate diesters (Chart 1, Compounds **1**–**4**) [66]. Hydrolytic reaction occurs due to the Lewis acid activation of the substrate by coordination with the metal ion and subsequent reaction with a water/hydroxyl group coordinated with the metal catalyst. In this case, a bimetallic mechanism is invoked. In particular, the two metal centers coordinate two oxygen atoms of the phosphoric group, and a hydroxyl group (initially bonded to the metal catalyst) attacks the organophosphorus substrate leading to the hydrolysis.

In addition, the chemoselectivity is due to the different metal ions able to hydrolyze different bonds: the ester bond C-OR is cleaved by Ce(IV) and Th(IV), while phospho-ester bond is cleaved by Zr(IV) and Hf(IV). In both cases, the authors detected the same leaving groups (–CH$_3$ or –Ph).

To understand the hydrolytic mechanism, they consider an intermediate where the selectivity of Zr(IV) and Hf(IV) toward phospho-ester bond is due to the formation of octameric or tetrameric complexes between the metal ion and the substrate. In some cases, such as with compound **3**, C–OPh ester bond hydrolysis occurs with respect to P–OMe, due to the modification of the catalyst-substrate complex geometry.

Lewis et al. reported the methanolysis of the methylphosphonate compounds **5**–**10** (see Chart 1), by using La^{3+} and Zn^{2+} complexes [67].

A comparison of the reactivity between phosphonate and phosphate triesters shows that the former are ca. 100-fold more reactive than the latter, also containing the same leaving groups. The catalysis is highly efficient, although in mild conditions (near to neutrality). Reaction occurs due to the activation of the substrate by Lewis acid-base interaction, followed by the methoxide attack to the phosphorous center.

The most reactive compound is methylphosphonate 5, in which the acceleration rate depends on the alkaline conditions (in the range ca. 10^6–10^7-fold). Conversely, the least reactive compound is methylphosphonate 10, with an increase of the rate of ca. 10^4–10^5-fold.

Brown and co-workers applied the same reactions to phosphonothioate compounds **17**–**21**, obtaining good results in terms of acceleration rates at room temperature and pH values [68].

Notably, the authors describe that a VX analogue can be methanolyzed at 25 °C in the presence of 1 mM of La^{3+} catalyst with a t$_{1/2}$ less than 1 s.

　　　Kuo et al. reported the catalytic degradation of *O,S*-diethyl phenylphosphonothioate 22 (DEPP, Chart 1), a simulant of neurotoxins, including VX, in mild conditions by using a metallocene catalyst (bis(η5-cyclopentadienyl)molybdenum(IV) dichloride, Cp$_2$MoCl$_2$) [69].

　　　The authors proposed a mechanism in which the substrate coordinates the metal catalyst by using both P=O and S atoms, thus activating the nucleophilic attack of a water molecule (or OH$^-$ in alkaline conditions) to the phosphorous metal center, with a mechanism very similar those reported in Scheme 2 (monometallic catalyst). Faster reactions were obtained increasing the electrophilicity of the metal center, by introducing in the cyclopentadienyl ligand two methyl groups.

　　　Singh and et al. reported a micellar system, by self-assembly of benzimidazolium receptor and an anionic surfactant (Scheme 3A), able to detect, by fluorescence measurements, the presence of the NA (diethylchlorophosphate, DCP) which then led to its degradation into non-toxic diethylhydrophosphate (DHP) (Scheme 3B) [70].
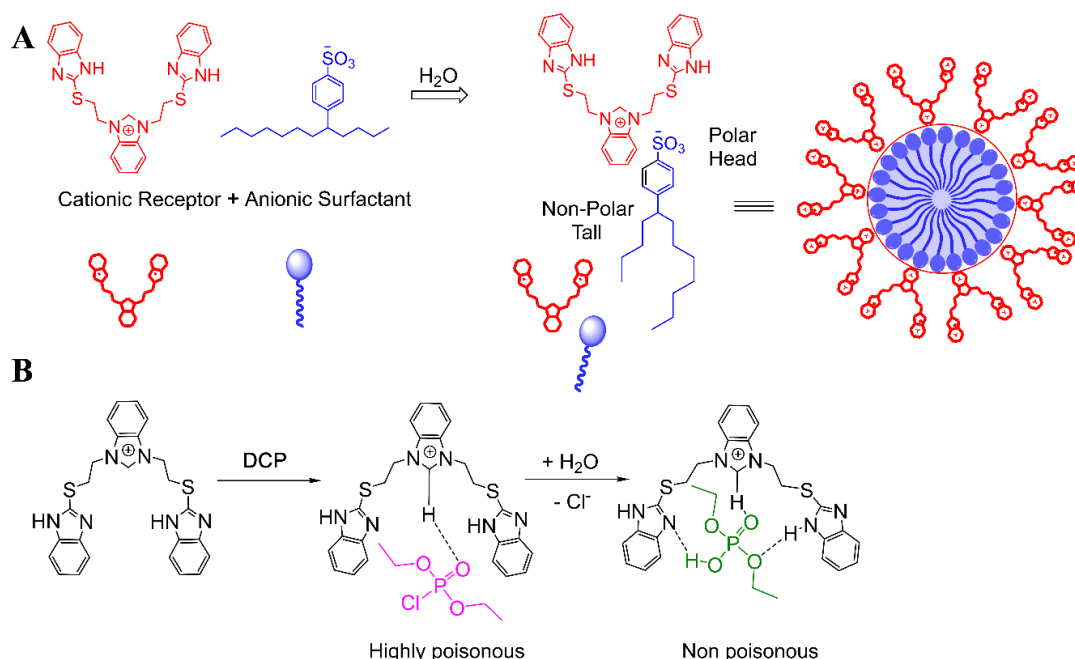

Scheme 3. (**A**) Schematic representation of micellar assembly, able also to recognize DCP; and (**B**) catalytic hydrolysis of DCP.

　　　The benzimidazolium receptor is able to recognize DCP by non-covalent interactions (Scheme 3B), leading to a strong turn-on of the emission due to an increase of the rigidity of the complex with DCP with respect to the starting sensor. The formation of the host–guest complex leads to the activation of the P=O group, due to the formation of a strong hydrogen bond. The degradation reaction was monitored by GC-MS, forming tetraethyldiphosphate (TDP) as an intermediate, which completely evolves into DHP in 1 h.

5.2. Polymeric/Heterogeneous Hydrolysis

　　　Chang et al. reported the synthesis of a polymer based on TRIM building block, containing copper as the metal-center catalyst and its catalytic activity towards the hydrolysis of some phosphate esters (Scheme 4) [71].
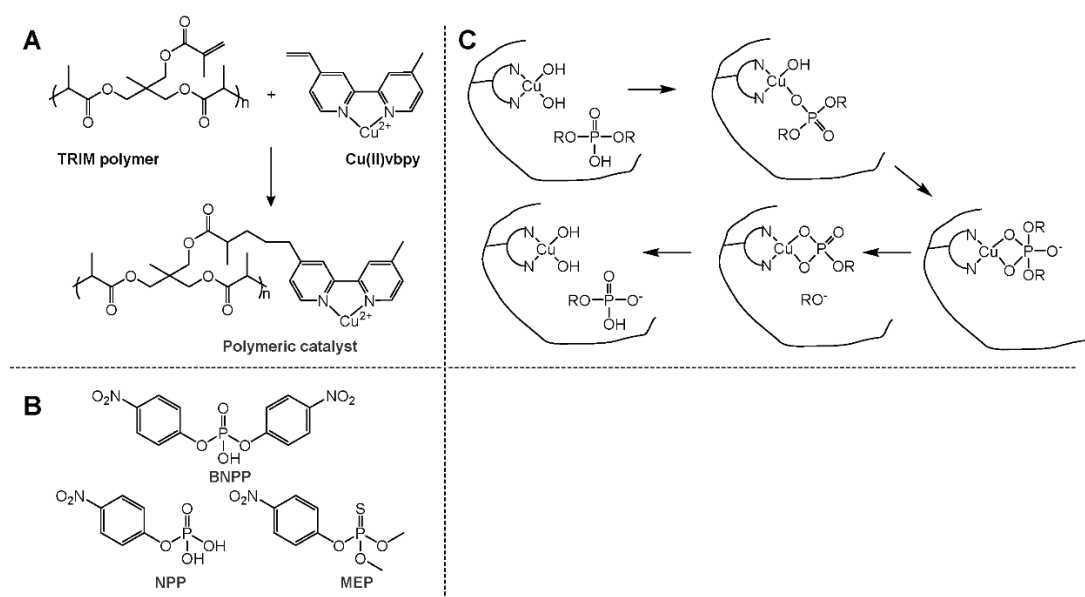
Scheme 4. (**A**) Synthesis and chemical structure of Cu-TRIM catalyst; (**B**) substrates tested; and (**C**) mechanism of hydrolysis.

In particular, hydrolysis of NPP, BNPP and MEP (Scheme 4B) was accelerated by the polymeric catalyst of 580, 2.5×10^4 and 6.7×10^5-fold, respectively, with respect to the uncatalyzed reaction. As reported in Scheme 4C, firstly the substrate coordinates the metal ion by removing a water molecule, then the intramolecular nucleophilic attack by a second water molecule bonded to the metal ion occurs, thus leading to a four-member cycle, which undergoes the elimination of the alkoxide substituent. Further reorganization of the cyclic intermediate leads to the hydrolysis product, recovering the starting catalyst. Thus, this polymer represents an efficient heterogeneous catalyst able to hydrolyze phosphate esters.

Brown et al. reported the methanolysis of some phosphor-esters (Compounds **6**, **17**, **23** and **24** in Chart 1) catalyzed by solid support containing lanthanide ions (La^{3+}, Sm^{3+}, Eu^{3+} and Yb^{3+}), in alkaline conditions [72].

Solid supports have been synthesized starting from commercial chlorobenzyl silica gel and polystyrene functionalized with iminodiacetic acid (IDA) and ethylenediamine-*N*,*N'*-diacetic acid (EDDA), in the presence of Ln^{3+} metal ions. With respect to the uncatalyzed reactions in the presence of methoxide anion, hydrolyses of 6 and 23 are about 8.5×10^5- and 1.76×10^6-fold faster, respectively. Similarly, increase of the reactions with 17 and 24 are 6.3×10^5- and 5×10^8-fold with respect to the uncatalyzed reactions. Solid catalysts containing Eu and Yb ions have been recycled many times without loss of reactivity. Based on the previous work [73], the authors proposed a monometallic mechanism, as summarized in Scheme 2. In the first step, the substrate coordinates metal center by Lewis acid-base interaction, thus activating the P=O group, then a nucleophilic attack of the methoxide to the P atom occurs, leading to a four-member ring, which results in the releasing of hydrolyzed organophosphorus product restoring the catalyst by addition of methanol (solvent).

5.3. Enzymatic Hydrolysis

Hydrolytic enzymes (organophosphorus hydrolase) can catalyze the hydrolysis of NAs, however the main limitation is related to the decrease of the pH of the reaction environment, due to the acidic nature of the hydrolysis products (for example, most of G-Type NAs release HF after the hydrolysis). In general, enzymatic efficiency decreases at pH values of <6 [74].

To avoid this problem, buffers may be used to maintain a neutral pH. In addition, some enzymes lead to the formation of ammonia starting from urea and can be used to control the pH levels [75].

In this way, by combining the two enzymes, organophosphorus hydrolase to hydrolyze the NA and urease to maintain the pH conditions, good conversion values can be obtained without loss of efficiency.

Enzymatic hydrolysis also exhibits the problem of the transport of the NA into the active site of the enzyme. To overcome this problem, catalytic enzymes have been anchored onto the surface of bacteria, and the whole system has been exposed to the NA. In particular, Mulchandani et al. reported on the coupling of DNA able to codify the organophosphorus hydrolase enzyme to the DNA able to codify some proteins of the cell surface [76]. With this strategy, several bacterial lines which have the catalytic enzyme on their surface can be obtained.

Following the same methodology, Mulchandani et al. also developed engineered *E. coli* bacteria, which have a cellulose-binding domain on the cellular surface, in order to create a reactor based on common fibers containing these nanocatalysts (Figure 3) [77]. This system was employed to catalyze the paraoxon hydrolysis in seven weeks, with the device being reused 15 times.
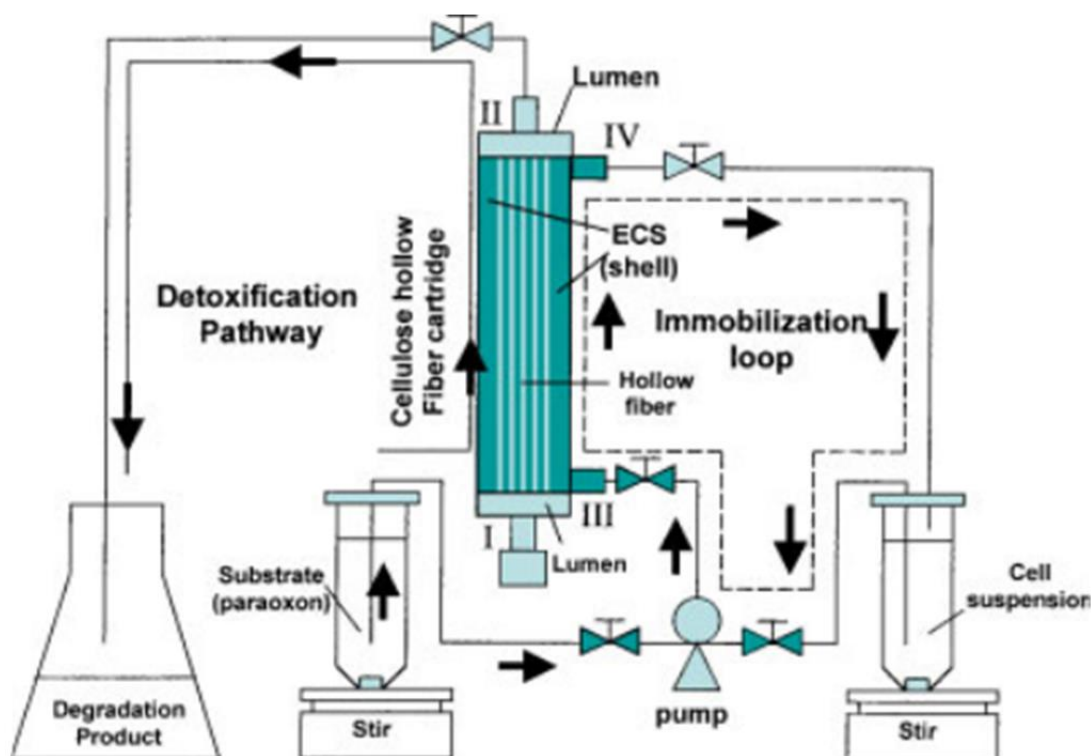

Figure 3. Schematic representation of the reactor based on cellulose nanocatalyst (reproduced with permission from *Biotechnol. Bioeng.* **2005**, *91*, 379–386. Copyright 2005 John Wiley and Sons).

In addition, several different classes of enzymes are able to hydrolyze organophosphorus compounds. In particular, Phosphotriesterases (PTE), containing a binuclear zinc or cobalt center in the active site, catalyze the hydrolysis of Sarin, Soman, Tabun and Cyclosarin, as well as VX and VR [78,79]. Furthermore, Serum paraoxonase 1 (PON1), a mammalian calcium-dependent lactonase/arylesterases, is able to hydrolyze G-Type NAs [80–82]. In addition, Diisopropyl-fluorophosphate fluorohydrolase (DFPase) hydrolyzes Tabun, Soman and Sarin [83]. Recently, Phosphotriesterase-like lactonase (PLL) enzymes have been discovered to hydrolyze some OP, and in particular cyclosarin [84].

5.4. Hydrolysis by MOFs

MOFs are a new class of porous nanomaterials. They present high surface area and internal volume, suitable for many interesting applications [9–13,85–103]. Building blocks are metal ions, having different coordination geometries, and a large range of organic ligands. For this reason, a wide typology of structures can be obtained [104–111].

Due to their three-dimensional structures, these nanoscopic compounds can be used as sensors for small and large molecules. The typical characteristics of MOFs are the extensive surface area (up to 1000 m^2/g), the huge number of reactive sites having potential catalytic activity, the possibility to regulate the pore sizes and the inner volume (by using different metal ions and organic ligands), and tune the catalytic properties regulating the nature of the metal ions.

Catalytic hydrolyses of NAs by MOFs are inspired by the enzyme-catalyzed hydrolysis of phosphor-ester substrates, in which a Zn ion leads to the activation of P=O group, facilitating the nucleophilic attack of the water molecule. In this context, Kats et al. reported the synthesis of based biomimetic MOFs containing Zr, able to hydrolyze NAs, in particular the methyl paraoxon and *p*-nitrophenyl diphenyl phosphate [112]. Similarly, Wagner and Peterson reported on the ability of a copper-based MOF (CuBTC) to hydrolyze VX and Soman in a matter of hours [113].

More efficient systems have been synthesized. Nunes and co-workers prepared UiO-67 MOF able to degrade ca. 90% of Sodium para-nitrophenylphosphate (a simulant of Soman) by simple filtration of NAs solution through the MOF [114].

Farha and co-workers synthesized different MOFs, tuning the linker between the metal center [115]. They established that the linker size and functional groups (amine or alkylamino) can strongly modulate the reactivity towards the hydrolysis of the NA. In particular, hydrolysis of 4-nitrophenylphosphate buffered at pH 10 occurred in only a few minutes by using the smaller MOFs containing amino groups in the linker. The reaction was monitored by using NMR and UV–Vis spectroscopies. In addition, the authors tested the catalytic degradation of Soman but, in this case, the reaction is too much fast to obtain information on the effect of the substituent of the MOF linker.

Recently, the same research group developed a composite material, integrating MOFs into a polymeric matrix (linear polyethylenimine), able to efficiently destroy DMNP and GD in mild conditions in the presence of an organic volatile base (*N*-ethyl morpholine), obtaining a solid device suitable for the decontamination from NAs (Figure 4) [116].
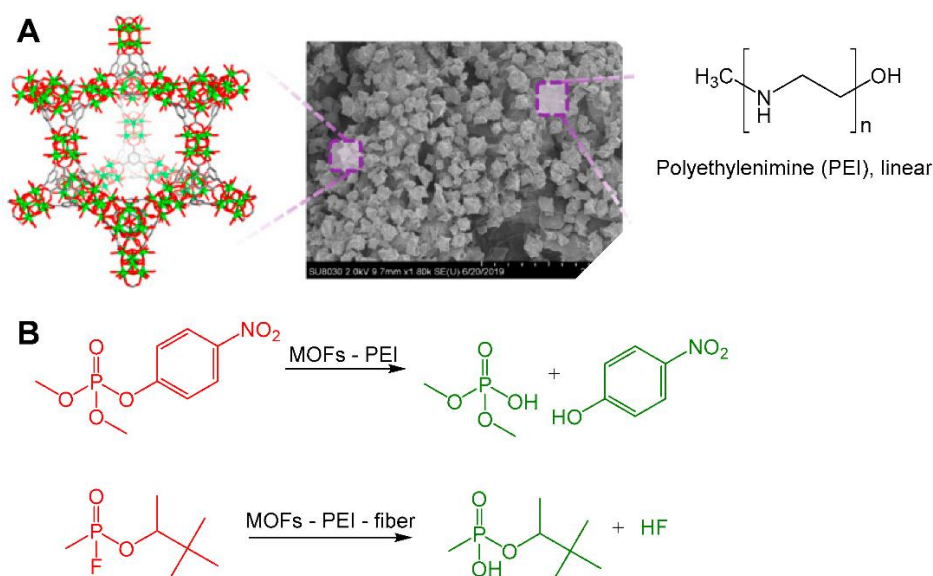

Figure 4. (**A**) Representation of MOF-808, PEI and image of the composite; and (**B**) degradation reaction of DMNP (adapted with permission from *J. Am. Chem. Soc.* **2019**, *141*, 20016–20021. Copyright 2019 American Chemical Society).

In particular, the authors demonstrated that the MOF pores contain only water molecules during the catalytic process, highlighting higher activity with respect to the other MOF systems in a water environment. Robustness and durability have been demonstrated, by stirring the sample in water for 24 h, observing the maintaining of the crystalline structure and the quantitative composition.

Furthermore, the catalytic properties are retained following storage in air for 100 days. In addition, scalability of the system was tested with good results, by testing a larger surface of the device.

Cohen et al. described a library of 26 UiO-66 derivatives, combining five different ligands, leading to Multivariate MOF catalysts (MTV-MOFs), able to hydrolyze DMNP in basic conditions (pH = 8) [117]. These MTV-MOFs have been synthesized by including nine different ligands into a single MOF structure. MTV-MOF catalysts show higher efficiency with respect to the mixture of single MOFs in the degradation of DMNP (Figure 5). In particular, this new type of nanocatalysts is more efficient than MOFs containing the same ligand. However, the authors did not find a correlation between the electron nature of the substituent in the ligand (electron-donating or withdrawing) and the catalytic efficiency. We note that, in analogy with what was previously observed [115], the best results of catalytic efficiency have been found by using ligands containing amino and bromide groups.
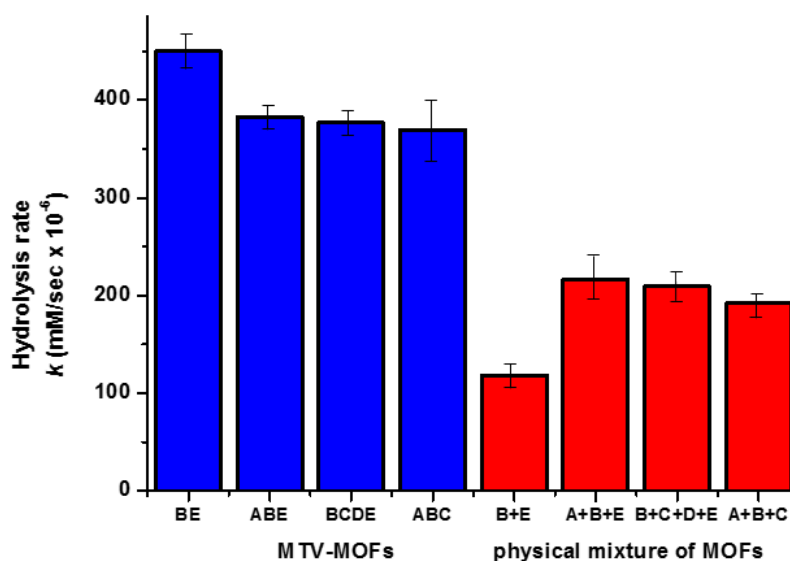

Figure 5. Chemical structure of the ligands employed to synthesize MTV-MOFs and hydrolysis rates of MTV-MOFs (in blue) and physical mixture of MOFs containing the same ligand (in red) (adapted with permission from *Chem. Commun.* **2019**, *55*, 5367–5370. Copyright 2019 Royal Society of Chemsitry).

6. Conclusions and Future Perspectives

Catalytic degradation methods of NAs by using molecular catalysts, both in homogeneous and heterogeneous conditions, enzymes and MOF systems are summarized. In most of the examples, simulants of NAs have been employed. This is for security reasons: as the use of real NAs is not allowed in most research laboratories, these tests are made with organophosphorus compounds having similar chemical characteristics with respect to the NAs. However, recently, DeCoste and Ploskonka focused their attention on the use of simulants against the real NAs in the study of hydrolysis processes [118]. They found that the reactivity of these simulants is not always comparable to the reactivity of the NAs, in particular by using nanoporous MOFs. In fact, they supposed that the reactivity inside the MOF structure is not only related to chemical interactions, but also steric factors should be considered. NAs show steric hindrance which, in many cases, differs with respect to that of the simulant used. However, these considerations are relative to the catalytic systems having restricted steric hindrances.

Due to the fast action mechanism of NAs to covalently bind AChE, the rate of NA degradation is a crucial parameter in order to avoid the lethal effects of these chemical weapons to the humans. For this reason, the implementation of molecular catalytic systems into heterogeneous of nanoscopic catalysts could be the goal to obtain efficient decontamination of the environment. As is well known, the possibility to realize solid porous surface/support containing a catalytic specie leads to an increase of the activity/reactivity, also obtaining a reusable device [119–121]. Scientific progresses in the field of

surfaces and nanoparticles functionalization improves the possibility of enhancing the results actually obtained with regard to NAs degradation.

Today, impressive research activity in material sciences, as well in nanoscience and enzymology leads to a greater chance of obtaining practical devices able to efficiently destroy nerve agents. In addition, the possibility of using these devices in public environments (such as airports, stations, schools and water systems) can potentially increase safety and security in protecting against terrorist attacks.

References

1.　Stone, R.U.K. Attack puts nerve agent in the spotlight. *Science* **2018**, *359*, 1314–1315. [CrossRef] [PubMed]

2.　Stone, R. How to defeat a nerve agent. *Science* **2018**, *359*, 23. [CrossRef] [PubMed]

3.　Haines, D.D.; Fox, S.C. Acute and Long-Term Impact of Chemical Weapons: Lessons from the Iran-Iraq War. *Forensic Sci. Rev.* **2014**, *26*, 97–114. [PubMed]

4.　Seto, Y.; Sekiguchi, H.; Maruko, H.; Yamashiro, S.; Sano, Y.; Takayama, Y.; Sekioka, R.; Yamaguchi, S.; Kishi, S.; Satoh, T.; et al. Sensitive and Comprehensive Detection of Chemical Warfare Agents in Air by Atmospheric Pressure Chemical Ionization Ion Trap Tandem Mass Spectrometry with Counterflow Introduction. *Anal. Chem.* **2014**, *86*, 4316–4326. [CrossRef]

5.　Bizzigotti, G.O.; Castelly, H.; Hafez, A.M.; Smith, W.H.B.; Whitmire, M.T. Parameters for Evaluation of the Fate, Transport, and Environmental Impacts of Chemical Agents in Marine Environments. *Chem. Rev.* **2009**, *109*, 236–256. [CrossRef]

6.　Valdez, C.A.; Leif, R.N.; Hok, S.; Hart, B.R. Analysis of chemical warfare agents by gas chromatography-mass spectrometry: Methods for their direct detection and derivatization approaches for the analysis of their degradation products. *Rev. Anal. Chem.* **2018**, *37*, 20170007. [CrossRef]

7.　Pacsial-Ong, E.J.; Aguilar, Z.P. Chemical warfare agent detection: A review of current trends and future perspective. *Front. Biosci.* **2013**, *5*, 516–543. [CrossRef]

8.　Picard, B.; Chataigner, I.; Maddaluno, J.; Legros, J. Introduction to chemical warfare agents, relevant simulants and modern neutralisation methods. *Org. Biomol. Chem.* **2019**, *17*, 6528–6537. [CrossRef]

9.　Liu, Y.; Howarth, A.J.; Vermeulen, N.A.; Moon, S.-Y.; Hupp, J.T.; Farha, O.K. Catalytic degradation of chemical warfare agents and their simulants by metal-organic frameworks. *Coord. Chem. Rev.* **2017**, *346*, 101–111. [CrossRef]

10.　Vellingiri, K.; Philip, L.; Kim, K. –H. Metal-organic frameworks as media for the catalytic degradation of chemical warfare agents. *Coord. Chem. Rev.* **2017**, *353*, 159–179. [CrossRef]

11.　Islamoglu, T.; Chen, Z.; Wasson, M.C.; Buru, C.T.; Kirlikovali, K.O.; Afrin, U.; Mian, M.R.; Farha, O.K. Metal-Organic Frameworks against Toxic Chemicals. *Chem. Rev.* **2020**. [CrossRef] [PubMed]

12.　Kirlikovali, K.O.; Chen, Z.; Islamoglu, T.; Hupp, J.T.; Farha, O.K. Zirconium-Based Metal—Organic Frameworks for the Catalytic Hydrolysis of Organophosphorus Nerve Agents. *ACS Appl. Mater. Interfaces* **2020**, *12*, 14702–14720. [CrossRef] [PubMed]

13.　Manco, G.; Porzio, E.; Suzumoto, Y. Enzymatic detoxification: A sustainable means of degrading toxic organophosphate pesticides and chemical warfare nerve agents. *J. Chem. Technol. Biotechnol.* **2018**, *93*, 2064–2082. [CrossRef]

14.　Singh, B.; Prasad, G.K.; Pandey, K.S.; Danikhel, R.K.; Vijayaraghavan, R. Decontamination of chemical warfare age. *Def. Sci. J.* **2010**, *60*, 428–441. [CrossRef]

15.　Wagner, G.W. Decontamination of Chemical Warfare Agents Using Household Chemica. *Ind. Eng. Chem. Res.* **2011**, *50*, 12285–12287. [CrossRef]

16. Costanzi, S.; Machado, J.-H.; Mitchell, M. Nerve Agents: What They Are, How They Work, How to Counter Them. *ACS Chem. Neurosci.* **2018**, *9*, 873–885. [CrossRef]

17. Vale, J.A.; Marrs, T.C.; Maynard, R.L. Novichok: A murderous nerve agent attack in the UK. *Clin. Toxicol.* **2018**, *56*, 1096–1097. [CrossRef]

18. Kloske, M.; Witkiewicz, Z. Novichoks—The A group of organophosphorus chemical warfare agents. *Chemosphere* **2019**, *221*, 672–682. [CrossRef]

19. Subramanyam, C.; Ramana, K.V.; Rasheed, S.; Adam, S.; Raju, C. Naga. Synthesis and Biological Activity of Novel Diphenyl N-Substituted Carbamimidoylphosphoramidate Derivatives. *Phosphorus Sulfur Silicon Relat. Elem.* **2013**, *188*, 1228–1235. [CrossRef]

20. Kuca, K.; Jun, D.; Musilek, K.; Bajgar, J. Reactivators of tabun-inhibited acetylcholinesterase: Structure-biological activity relationship. *Front. Drug Des. Discov.* **2007**, *3*, 381–394.

21. Abou-Donia, M.B.; Siracuse, B.; Gupta, N.; Sobel Sokol, A. Sarin (GB, O-isopropyl methylphosphonofluoridate) neurotoxicity: Critical review. *Crit. Rev. Toxicol.* **2016**, *46*, 845–875. [CrossRef] [PubMed]

22. van Helden, H.P.M.; Joosen, M.J.A.; Philippens, I.H.C. Non-enzymatic pretreatment of nerve agent (soman) poisoning: A brief state-of-the-art review. *Toxicol. Lett.* **2011**, *206*, 35–40. [CrossRef] [PubMed]

23. Krejcova, G.; Kuca, K.; Sevelova, L. Cyclosarin. An organophosphate nerve agent. *Def. Sci. J.* **2005**, *55*, 105–115. [CrossRef]

24. Ovenden, S.P.B.; Webster, R.L.; Micich, E.; McDowall, L.J.; McGill, N.W.; Williams, J.; Zanatta, S.D. The identification of chemical attribution signatures of stored VX nerve agents using NMR, GC-MS, and LC-HRM. *Talanta* **2020**, *211*, 120753. [CrossRef]

25. Ghanem, E.; Li, Y.; Xu, C.; Raushel, F.M. Characterization of a Phosphodiesterase Capable of Hydrolyzing EA 2192, the Most Toxic Degradation Product of the Nerve Agent VX. *Biochemistry* **2007**, *46*, 9032–9040. [CrossRef]

26. Witkiewicz, Z.; Neffe, S.; Sliwka, E.; Quagliano, J. Analysis of the precursors, simulants and degradation products of chemical warfare agents. *Crit. Rev. Anal. Chem.* **2018**, *48*, 337–371. [CrossRef]

27. Agrawal, M.; Gallis, D.F.S.; Greathouse, J.A.; Sholl, D. How Useful Are Common Simulants of Chemical Warfare Agents at Predicting Adsorption Behavior? *J. Phys. Chem. C* **2018**, *122*, 26061–26069. [CrossRef]

28. Tu, A.T. Aum Shinrikyo's Chemical and Biological Weapons: More Than Sarin. *Forensic Sci. Rev.* **2014**, *26*, 115–120.

29. Somani, S.M.; Solana, R.P.; Dube, S.N. Toxicodynamics of nerve agents. In *Chemical Warfare Agents*; Somani, S.M., Ed.; Academic Press: Cambridge, MA, USA, 1992; pp. 67–123.

30. Spradling, K.D.; Dillman, J.F. The molecular toxicology of chemical warfare nerve agents. In *Advances in Molecular Toxicology*; James, C.F., Ed.; Elsevier B.V.: Amsterdam, The Netherlands, 2011; pp. 111–144.

31. Mercey, G.; Verdelet, T.; Renou, J.; Kliachina, M.; Baati, R.; Nachon, F.; Jean, L.; Renard, P.-Y. *Acc. Chem. Res.* **2012**, *45*, 756–766. [CrossRef]

32. Ekström, F.; Hörnberg, A.; Artursson, E.; Hammarström, L.G.; Schneider, G.; Pang, Y.P. Structure of HI-6 *sarin-acetylcholinesterase determined by X-ray crystallography and molecular dynamics simulation: Reactivator mechanism and design. *PLoS ONE* **2009**, *4*, e5957. [CrossRef]

33. Rupa, I.; Brian, I.; Alex, L. Developments in alternative treatments for organophosphate poisoning. *Toxicol. Lett.* **2015**, *233*, 200–206.

34. Sidell, F.R. Soman and Sarin: Clinical manifestations and treatment of accidental poisoning by organophosphates. *Clin Toxicol.* **1974**, *7*, 1–17. [CrossRef] [PubMed]

35. Sidell, F.R.; Groff, W.A. The reactivatibility of cholinesterase inhibited by VX and Sarin in man. *Toxicol. Appl. Pharmacol.* **1974**, *27*, 241–252. [CrossRef]

36. Sidell, F.R.; Borak, J. Chemical warfare agents: II. Nerve agents. *Ann. Emerg. Med.* **1992**, *21*, 865–871. [CrossRef]

37. Noort, D.; Benschop, H.P.; Black, R.M. Biomonitoring of Exposure to Chemical Warfare Agents: A Review. *Toxicol. Appl. Pharm.* **2002**, *184*, 116–126. [CrossRef]

38. Ghanei, M.; Fathi, H.; Mohammad, M.M.; Aslani, J.; Nematizadeh, F. Long-Term Respiratory Disorders of Claimers with Subclinical Exposure to Chemical Warfare Agents. *Inhal. Toxicol.* **2004**, *16*, 491–495. [CrossRef]

39. Wiener, S.W.; Hoffman, R.S. Nerve Agents: A Comprehensive Review. *J. Intensive Care Med.* **2004**, *19*, 22–37. [CrossRef]

40. Baygildiev, T.; Vokuev, M.; Ogorodnikov, R.; Braun, A.; Rybalchenko, I.; Rodin, I. Simultaneous determination of organophosphorus nerve agent markers in urine by IC-MS/MS using anion-exchange solid-phase extraction. *J. Chrom. B* **2019**, *1132*, 121815. [CrossRef]

41. B'Hymer, C. A brief overview of HPLC-MS analysis of alkyl methylphosphonic acid degradation products of nerve agents. *J. Chrom. Sci.* **2019**, *57*, 606–617. [CrossRef]

42. Kim, H.; Cho, Y.; Lee, B.S.; Choi, I.S. In-situ derivatization and headspace solid-phase microextraction for gas chromatography-mass spectrometry analysis of alkyl methylphosphonic acids following solid-phase extraction using thin film. *J. Chrom. A* **2019**, *1599*, 17–24. [CrossRef]

43. Jang, Y.J.; Kim, K.; Tsay, O.G.; Atwood, D.A.; Churchill, D.G. Update 1 of: Destruction and Detection of Chemical Warfare Agents. *Chem. Rev.* **2015**, *115*, PR1–PR76. [CrossRef]

44. Chen, L.; Wu, D.; Yoon, J. Recent Advances in the Development of Chromophore-Based Chemosensors for Nerve Agents and Phosgene. *ACS Sens.* **2018**, *3*, 27–43. [CrossRef]

45. Dey, N.; Jha, S.; Bhattacharya, S. Visual detection of a nerve agent simulant using chemically modified paper strips and dye-assembled inorganic nanocomposite. *Analyst* **2018**, *143*, 528–535. [CrossRef]

46. Sambrook, M.R.; Notman, S. Supramolecular chemistry and chemical warfare agents: From fundamentals of recognition to catalysis and sensing. *Chem. Soc. Rev.* **2013**, *42*, 9251–9267. [CrossRef] [PubMed]

47. Border, S.E.; Pavlovic, R.Z.; Zhiquan, L.; Badjic, J.D. Removal of Nerve Agent Simulants from Water Using Light-Responsive Molecular Baskets. *J. Am. Chem. Soc.* **2017**, *139*, 18496–18499. [CrossRef] [PubMed]

48. Chen, S.; Ruan, Y.; Brown, J.D.; Hadad, C.M.; Badjic, J.D. Recognition Characteristics of an Adaptive Vesicular Assembly of Amphiphilic Baskets for Selective Detection and Mitigation of Toxic Nerve Agents. *J. Am. Chem. Soc.* **2014**, *136*, 17337–17342. [CrossRef] [PubMed]

49. Ruan, Y.; Dalkilic, E.; Peterson, P.W.; Pandit, A.; Dastan, A.; Brown, J.D.; Polen, S.M.; Hadad, C.M.; Badjic, J.D. Trapping of organophosphorus chemical nerve agents in water with amino acid functionalized baskets. *Chem. Eur. J.* **2014**, *20*, 4251–4256. [CrossRef] [PubMed]

50. Chen, S.; Ruan, Y.; Brown, J.D.; Gallucci, J.; Maslak, V.; Hadad, C.M.; Badjic, J.D. Assembly of Amphiphilic Baskets into Stimuli-Responsive Vesicles. Developing a Strategy for the Detection of Organophosphorus Chemical Nerve Agents. *J. Am. Chem. Soc.* **2013**, *135*, 14964–14967. [CrossRef] [PubMed]

51. Ha, S.; Lee, M.; Seo, H.O.; Song, S.G.; Kim, K.; Park, C.H.; Kim, I.L.; Kim, Y.D.; Song, C. Structural Effect of Thioureas on the Detection of Chemical Warfare Agent Simulants. *ACS Sens.* **2017**, *2*, 1146–1151. [CrossRef]

52. Hiscock, J.R.; Piana, F.; Sambrook, M.R.; Wells, N.J.; Clark, A.J.; Vincent, J.C.; Busschaert, N.; Brown, R.C.D.; Gale, P.A. Detection of nerve agent via perturbation of supramolecular gel formation. *Chem. Commun.* **2013**, *49*, 9119–9121. [CrossRef]

53. Esipenko, N.A.; Koutnik, P.; Minami, T.; Mosca, L.; Lynch, V.M.; Zyryanov, G.V.; Anzenbacher, P., Jr. First supramolecular sensors for phosphonate anions. *Chem. Sci.* **2013**, *4*, 3617–3623. [CrossRef]

54. Hiscock, J.R.; Sambrook, M.R.; Wells, N.J.; Gale, P.A. Detection and remediation of organophosphorus compounds by oximate containing organogels. *Chem. Sci.* **2015**, *6*, 5680–5684. [CrossRef]

55. Ishihara, S.; Azzarelli, J.M.; Krikorian, M.; Swager, T.M. Ultratrace Detection of Toxic Chemicals: Triggered Disassembly of Supramolecular Nanotube Wrappers. *J. Am. Chem. Soc.* **2016**, *138*, 8221–8227. [CrossRef]

56. Hiscock, J.R.; Wells, N.J.; Ede, J.A.; Gale, P.A.; Sambrook, M.R. Biasing hydrogen bond donating host systems towards chemical warfare agent recognition. *Org. Biomol. Chem.* **2016**, *14*, 9560–9567. [CrossRef] [PubMed]

57. Chung, Y.K.; Ha, S.; Woo, T.G.; Kim, Y.D.; Song, C.; Kim, S.K. Binding thiourea derivatives with dimethyl methylphosphonate for sensing nerve agents. *RSC Adv.* **2019**, *9*, 10693–10701. [CrossRef]

58. Kwon, O.S.; Park, C.S.; Park, S.J.; Noh, S.; Kim, S.; Kong, H.J.; Bae, J.; Lee, C.-S.; Yoon, H. Carboxylic Acid-Functionalized Conducting-Polymer Nanotubes as Highly Sensitive Nerve-Agent Chemiresistors. *Sci. Rep.* **2016**, *6*, 33724. [CrossRef]

59. Fennell, J.F., Jr.; Hamaguchi, H.; Yoon, B.; Swager, T.M. Chemiresistor Devices for Chemical Warfare Agent Detection Based on Polymer Wrapped Single-Walled Carbon Nanotubes. *Sensors* **2017**, *17*, 982. [CrossRef]

60. Pappalardo, A.; Amato, M.E.; Ballistreri, F.P.; La Paglia Fragola, V.; Tomaselli, G.A.; Toscano, R.M.; Sfrazzetto, G.T. Binding of reactive organophosphate by oximes via hydrogen bond. *J. Chem. Sci.* **2013**, *125*, 869–873. [CrossRef]

61. Sfrazzetto, G.T.; Millesi, S.; Pappalardo, A.; Tomaselli, G.A.; Ballistreri, F.P.; Toscano, R.M.; Fragalà, I.; Gulino, A. Nerve Gas Simulant Sensing by a Uranyl–Salen Monolayer Covalently Anchored on Quartz Substrates. *Chem. Eur. J.* **2017**, *23*, 1576–1583. [CrossRef]

62. Puglisi, R.; Mineo, P.G.; Pappalardo, A.; Gulino, A.; Sfrazzetto, G.T. Supramolecular Detection of a Nerve Agent Simulant by Fluorescent Zn–Salen Oligomer Receptors. *Molecules* **2019**, *24*, 2160. [CrossRef]

63. Puglisi, R.; Pappalardo, A.; Gulino, A.; Sfrazzetto, G.T. Supramolecular recognition of a CWA simulant by metal–salen complexes: The first multi-topic approach. *Chem. Comm.* **2018**, *54*, 11156–11159. [CrossRef] [PubMed]

64. Puglisi, R.; Pappalardo, A.; Gulino, A.; Sfrazzetto, G.T. Multitopic Supramolecular Detection of Chemical Warfare Agents by Fluorescent Sensors. *ACS Omega* **2019**, *4*, 7550–7555. [CrossRef]

65. Legnani, L.; Puglisi, R.; Pappalardo, A.; Chiacchio, M.A.; Sfrazzetto, G.T. Supramolecular recognition of phosphocholine by an enzyme-like cavitand receptor. *Chem. Commun.* **2020**, *56*, 539–542. [CrossRef] [PubMed]

66. Moss, R.A.; Morales-Rojas, H.; Vijayaraghavan, S.; Tian, J.Z. Metal-Cation-Mediated Hydrolysis of Phosphonoformate Diesters: Chemoselectivity and Catalysis. *J. Am. Chem. Soc.* **2004**, *126*, 10923–10963. [CrossRef]

67. Lewis, R.E.; Neverov, A.A.; Brown, R.S. Mechanistic studies of La^{3+} and Zn^{2+}-catalyzed methanolysis of O-ethyl O-aryl methylphosphonate esters. An effective solvolytic method for the catalytic destruction of phosphonate CW simulants. *Org. Biomol. Chem.* **2005**, *3*, 4082–4088. [CrossRef]

68. Melnychuk, S.A.; Neverov, A.A.; Brown, R.S. Catalytic decomposition of simulants for chemical warfare V agents: Highly efficient catalysis of the methanolysis of phosphonothioate esters. *Angew. Chem., Int. Ed.* **2006**, *45*, 1767–1770. [CrossRef]

69. Kuo, L.Y.; Adint, T.T.; Akagi, A.E.; Zakharov, L. Degradation of a VX Analogue: First Organometallic Reagent To Promote Phosphonothioate Hydrolysis Through Selective P-S Bond Scission. *Organometallics* **2008**, *27*, 2560–2564. [CrossRef]

70. Singh, A.; Raj, P.; Singh, N. Benzimidazolium-Based Self-Assembled Fluorescent Aggregates for Sensing and Catalytic Degradation of Diethylchlorophosphate. *ACS Appl. Mater. Interfaces* **2016**, *8*, 28641–28651. [CrossRef]

71. Hartshorn, C.M.; Singh, A.; Chang, E.L. Metal-chelator polymers as organophosphate hydrolysis catalys. *J. Mater. Chem.* **2002**, *12*, 602–605. [CrossRef]

72. Andrea, T.; Neverov, A.A.; Brown, R.S. Efficient Methanolytic Cleavage of Phosphate, Phosphonate, and Phosphonothioate Esters Promoted by Solid Supported Lanthanide Ions. *Ind. Eng. Chem. Res.* **2010**, *49*, 7027–7033. [CrossRef]

73. Desloges, W.; Neverov, A.A.; Brown, R.S. Zn^{2+}-Catalyzed Methanolysis of Phosphate Triesters: A Process for Catalytic Degradation of the Organophosphorus Pesticides Paraoxon and Fenitrothion. *Inorg. Chem.* **2004**, *43*, 6752–6761. [CrossRef] [PubMed]

74. Smith, B.M. Catalytic methods for the destruction of chemical warfare agents under ambient conditions. *Chem. Soc. Rev.* **2008**, *37*, 470–478. [CrossRef] [PubMed]

75. Russell, A.J.; Erbeldinger, M.; DeFrank, J.J.; Kaar, J.; Drevon, G. Catalytic buffers enable positive-response inhibition-based sensing of nerve agents. *Biotechnol. Bioeng.* **2002**, *77*, 352–357. [CrossRef] [PubMed]

76. Takayama, K.; Suye, S.-I.; Kuroda, K.; Ueda, M.; Kitaguchi, T.; Tsuchiyama, K.; Fukuda, T.; Chen, W.; Mulchandani, A. Surface Display of Organophosphorus Hydrolase on Saccharomyces cerevisiae. *Biotechnol. Prog.* **2006**, *22*, 939–943. [CrossRef]

77. Wang, A.A.; Chen, W.; Mulchandani, A. Detoxification of organophosphate nerve agents by immobilized dual functional biocatalysts in a cellulose hollow fiber bioreactor. *Biotechnol. Bioeng.* **2005**, *91*, 379–386. [CrossRef]

78. Dumas, D.P.; Durst, H.D.; Landis, W.G.; Raushel, F.M.; Wild, J.R. Inactivation of organophosphorus nerve agents by the phosphotriesterase from Pseudomonas diminuta. *Arch. Biochem. Biophys.* **1990**, *277*, 155–159. [CrossRef]

79. Kolakowski, J.E.; Defrank, J.J.; Harvey, S.P.; Szafraniec, L.L.; Beaudry, W.T.; Lai, K.; Wild, J.R. Enzymatic hydrolysis of the chemical warfare agent VX and its neurotoxic analogues by organophosphorus hydrolase. *Biocatal. Biotransform* **1997**, *15*, 297–312. [CrossRef]

80. Mackness, M.I.; Arrol, S.; Durrington, P. Substrate specificity of human serum paraoxonase. *Biochem. Soc. Trans.* **1991**, *19*, 304S. [CrossRef]

81. Furlong, C.E.; Richter, R.J.; Chapline, C.; Crabb, J.W. Purification of rabbit and human serum paraoxonase. *Biochemistry* **1991**, *30*, 10133–10140. [CrossRef]

82. Li, W.F.; Furlong, C.E.; Costa, L.G. Paraoxonase protects against chlorpyrifos toxicity in mice. *Toxicol. Lett.* **1995**, *76*, 219–226. [CrossRef]

83. Hoskin, F.C. Diisopropylphosphorofluoridate and Tabun: Enzymatic hydrolysis and nerve function. *Science* **1971**, *172*, 1243–1245. [CrossRef] [PubMed]

84. Merone, L.; Mandrich, L.; Porzio, E.; Rossi, M.; Muller, S.; Reiter, G.; Worek, F.; Manco, G. Improving the promiscuous nerve agent hydrolase activity of a thermostable archaeal lactonase. *Bioresour. Technol.* **2010**, *101*, 9204–9212. [CrossRef] [PubMed]

85. Motkuri, R.K.; Thallapally, P.K.; Annapureddy, H.V.; Dang, L.X.; Krishna, R.; Nune, S.K.; Fernandez, C.A.; Liu, J.; McGrail, B.P. Separation of polar compounds using a flexible metal-organic framework. *Chem. Commun.* **2015**, *51*, 8421–8424. [CrossRef] [PubMed]

86. Nugent, P.; Belmabkhout, Y.; Burd, S.D.; Cairns, A.J.; Luebke, R.; Forrest, K.; Pham, T.; Ma, S.; Space, B.; Wojtas, L.; et al. Porous materials with optimal adsorption thermodynamics and kinetics for CO_2 separation. *Nature* **2013**, *495*, 80–84. [CrossRef]

87. Motkuri, R.K.; Thallapally, P.K.; Nune, S.K.; Fernandez, C.A.; McGrail, B.P.; Atwood, J.L. Role of hydrocarbons in pore expansion and contraction of a flexible metalorganic framework. *Chem. Commun.* **2011**, *47*, 7077–7079. [CrossRef]

88. Wilmer, C.E.; Farha, O.K.; Yildirim, T.; Eryazici, I.; Krungleviciute, V.; Sarjeant, A.A.; Snurr, R.Q.; Hupp, J.T. Gram-scale, High-yield Synthesis of a Robust Metal–Organic Framework for Storing Methane and Other Gases. *Energ. Environ. Sci.* **2013**, *6*, 1158–1163. [CrossRef]

89. Motkuri, R.K.; Annapureddy, H.V.R.; Vijaykumar, M.; Schaef, H.T.; Martin, P.F.; McGrail, B.P.; Dang, L.X.; Krishna, R.; Thallapally, P.K. Fluorocarbon adsorption in hierarchical porous frameworks. *Nat. Commun.* **2014**, *5*, 4368. [CrossRef]

90. An, J.; Farha, O.K.; Hupp, J.T.; Pohl, E.; Yeh, J.I.; Rosi, N.L. Metal-adeninate vertices for the construction of an exceptionally porous metal-organic framework. *Nat. Commun.* **2012**, *3*, 604. [CrossRef]

91. Motkuri, R.K.; Thallapally, P.K.; McGrail, B.P.; Ghorishi, S.B. Dehydrated Prussian Blues for CO_2 Storage and Separation Applications. *CrystEngComm* **2010**, *12*, 4003–4006. [CrossRef]

92. Thallapally, P.K.; Motkuri, R.K.; Fernandez, C.A.; McGrail, B.P.; Behrooz, G.S. Prussian blue analogues for CO_2 and SO_2 capture and separation applications. *Inorg. Chem.* **2010**, *49*, 4909–4915. [CrossRef]

93. Corma, A.; García, H.; Xamena, F.X.L.I. Engineering metal organic frameworks for heterogeneous catalysis. *Chem. Rev.* **2010**, *110*, 4606–4655. [CrossRef] [PubMed]

94. Chen, B.; Yang, Y.; Zapata, F.; Lin, G.; Qian, G.; Lobkovsky, E.B. Luminescent Open Metal Sites within a Metal–Organic Framework for Sensing Small Molecules. *Adv. Mater.* **2007**, *19*, 1693–1696. [CrossRef]

95. Chen, B.L.; Xiang, S.C.; Qian, G.D. Metal-Organic Frameworks with Functional Pores for Recognition of Small Molecules. *Acc. Chem. Res.* **2010**, *43*, 1115–1124. [CrossRef] [PubMed]

96. DeCoste, J.B.; Peterson, G.W. Metal-organic frameworks for air purification of toxic chemicals. *Chem. Rev.* **2014**, *114*, 5695–5727. [CrossRef]

97. Barea, E.; Montoro, C.; Navarro, J.A. Toxic gas removal–metal-organic frameworks for the capture and degradation of toxic gases and vapours. *Chem. Soc. Rev.* **2014**, *43*, 5419–5430. [CrossRef]

98. López-Maya, E.; Montoro, C.; Rodríguez-Albelo, L.M.; Cervantes, S.D.A.; Lozano-Pérez, A.A.; Cenis, J.L.; Barea, E.; Navarro, J.A.R. Textile/Metal-organic-framework composites as self-detoxifying filters for chemical-warfare agents. *Angew. Chem. Int. Ed.* **2015**, *54*, 6790–6794. [CrossRef]

99. Bromberg, L.; Klichko, Y.; Chang, E.P.; Speakman, S.; Straut, C.M.; Wilusz, E.; Hatton, T.A. Alkylaminopyridine-modified aluminum aminoterephthalate metal-organic frameworks as components of reactive self-detoxifying materials. *ACS Appl. Mater. Interfaces* **2012**, *4*, 4595–4602. [CrossRef]

100. Kitagawa, S.; Kitaura, R.; Noro, S. Functional porous coordination polymers. *Angew. Chem. Int. Ed.* **2004**, *43*, 2334–2375. [CrossRef]

101. Rowsell, J.L.C.; Yaghi, O.M. Metal–organic frameworks: A new class of porous materials. *Micropor. Mesopor. Mat.* **2004**, *73*, 3–14. [CrossRef]

102. Mondloch, J.E.; Katz, M.J.; Isley, W.C.; Ghosh, P.; Liao, P.L.; Bury, W.; Wagner, G.W.; Hall, M.G.; DeCoste, J.B.; Peterson, G.W.; et al. Destruction of chemical warfare agents using metal–organic frameworks. *Nat. Mater.* **2015**, *14*, 512–516. [CrossRef]

103. Greathouse, J.A.; Ockwig, N.W.; Criscenti, L.J.; Guilinger, T.R.; Pohl, P.; Allendorf, M.D. Computational screening of metal-organic frameworks for large-molecule chemical sensing. *Phys. Chem. Chem. Phys.* **2012**, *12*, 12621–12629. [CrossRef] [PubMed]

104. Chae, H.K.; Siberio-Perez, D.Y.; Kim, J.; Go, Y.B.; Eddaoudi, M.; Matzger, A.J.; O'Keeffe, M.; Yaghi, O.M. A route to high surface area, porosity and inclusion of large molecules in crystals. *Nature* **2004**, *427*, 523–527. [CrossRef] [PubMed]

105. Lee, J.; Farha, O.K.; Roberts, J.; Scheidt, K.A.; Nguyen, S.T.; Hupp, J.T. Metal-organic framework materials as catalysts. *Chem. Soc. Rev.* **2009**, *38*, 1450–1459. [CrossRef] [PubMed]

106. Lee, J.Y.; Farha, O.K.; Roberts, J.; Scheidt, K.A.; Nguyen, S.B.T.; Hupp, J.T. A chromium terephthalate-based solid with unusually large pore volumes and surface area. *Science* **2005**, *309*, 2040–2042.

107. Motkuri, R.K.; Liu, J.; Fernandez, C.A.; Nune, S.K.; Thallapally, P.; McGrail, B.P. Metal-Organic Frameworks -Synthesis and Applications. In *Chapter 3 in Industrial Catalysis and Separations: Innovations for Process Intensification*; Apple Academic Press: Waretown, NJ, USA, 2014; pp. 61–103.

108. Feng, D.; Wang, K.; Su, J.; Liu, T.-F.; Park, J.; Wei, Z.; Bosch, M.; Yakovenko, A.; Zou, X.; Zhou, H.-C. A highly stable zeotype mesoporous zirconium metal-organic framework with ultralarge pores. *Angew. Chem. Int. Ed.* **2015**, *54*, 149–154. [CrossRef]

109. Lee, Y.R.; Kim, J.; Ahn, W.S. Synthesis of metal-organic frameworks: A mini review. *Korean J. Chem. Eng.* **2013**, *30*, 1667–1680. [CrossRef]

110. Furukawa, H.; Cordova, K.E.; O'Keeffe, M.; Yaghi, O.M. The chemistry and applications of metal-organic frameworks. *Science* **2013**, *341*, 974. [CrossRef]

111. Conato, M.T.; Oleksiak, M.D.; McGrail, B.P.; Motkuri, R.K.; Rimer, J.D. Framework stabilization of Si-rich LTA zeolite prepared in organic-free media. *Chem. Commun.* **2015**, *51*, 269–272. [CrossRef]

112. Katz, M.J.; Mondloch, J.E.; Totten, R.K.; Park, J.K.; Nguyen, S.B.T.; Farha, O.K.; Hupp, J.T. Simple and compelling biomimetic metal-organic framework catalyst for the degradation of nerve agent simulants. *Angew. Chem. Int. Ed.* **2014**, *53*, 497–501. [CrossRef]

113. Peterson, G.W.; Wagner, G.W. Detoxification of chemical warfare agents by CuBTC. *J. Porous Mater.* **2014**, *21*, 121–126. [CrossRef]

114. Nunes, P.; Gomes, A.C.; Pillinger, M.; Goncalves, I.S.; Abrantes, M. Promotion of phosphoester hydrolysis by the ZrIV-based metal-organic framework UiO-67. *Micropor. Mesopor. Mat.* **2015**, *208*, 21–29. [CrossRef]

115. Peterson, G.W.; Moon, S.-Y.; Wagner, G.W.; Hall, M.G.; DeCoste, J.B.; Hupp, J.T.; Farha, O.K. Tailoring the Pore Size and Functionality of UiO-Type Metal-Organic Frameworks for Optimal Nerve Agent Destruction. *Inorg. Chem.* **2015**, *54*, 9684–9686. [CrossRef] [PubMed]

116. Chen, Z.; Ma, K.; Mahle, J.J.; Wang, H.; Syed, Z.H.; Atilgan, A.; Chen, Y.; Xin, J.H.; Islamoglu, T.; Peterson, G.W.; et al. Integration of Metal-Organic Frameworks on Protective Layers for Destruction of Nerve Agents under Relevant Conditions. *J. Am. Chem. Soc.* **2019**, *141*, 20016–20021. [CrossRef] [PubMed]

117. Kalaj, M.; Palomba, J.M.; Bentz, K.C.; Cohen, S.M. Multiple functional groups in UiO-66 improve chemical warfare agent simulant degradation. *Chem. Commun.* **2019**, *55*, 5367–5370. [CrossRef] [PubMed]

118. Ploskonka, A.B.; DeCoste, J.B. Insight into organophosphate chemical warfare agent simulant hydrolysis in metal-organic frameworks. *J. Haz. Mat.* **2019**, *375*, 191–197. [CrossRef]

119. Zammataro, A.; Gangemi, C.M.A.; Pappalardo, A.; Toscano, R.M.; Puglisi, R.; Nicotra, G.; Fragalà, M.E.; Tuccitto, N.; Trusso Sfrazzetto, G. Covalently functionalized carbon nanoparticles with a chiral Mn-Salen: A new nanocatalyst for enantioselective epoxidation of alkenes. *Chem. Commun.* **2019**, *55*, 5255–5258. [CrossRef]

120. Sfrazzetto, G.T.; Millesi, S.; Pappalardo, A.; Toscano, R.M.; Ballistreri, F.P.; Tomaselli, G.A.; Gulino, A. Olefin Epoxidation by a (salen) Mn(III) Catalyst Covalently Grafted on Glass Beads. *Cat. Sci. Techn.* **2015**, *5*, 673–679. [CrossRef]

121. La Paglia Fragola, V.; Lupo, F.; Pappalardo, A.; Sfrazzetto, G.T.; Toscano, R.M.; Ballistreri, F.P.; Tomaselli, G.A.; Gulino, A. A surface-confined O=MnV(salen) oxene catalyst and high turnover values in asymmetric epoxidation of unfunctionalized olefins. *J. Mater. Chem.* **2012**, *22*, 20561–20565. [CrossRef]